SAND2016-8913C

Material Identification with Multichannel Radiographs

Noelle Collins[1, a)] , Dr. Edward S. Jimenez[1, b)], and Kyle R. Thompson[1, c)]

[1] *Sandia National Laboratories, MS 0615, Albuquerque, NM 87185-0615*

[a)]Corresponding author: nmcolli@sandia.gov
[b)]esjimen@sandia.gov
[c)] krthomp@sandia.gov

Abstract. This work aims to validate previous exploratory work done to characterize materials by matching their attenuation profiles using a multichannel radiograph given an initial energy spectrum [1][2][3]. The experiment was performed in order to evaluate the effects of noise on the resulting attenuation profiles, which was ignored in simulation. Spectrum measurements have also been collected from various materials of interest. Additionally, a MATLAB optimization algorithm has been applied to these candidate spectrum measurements in order to extract an estimate of the attenuation profile. Being able to characterize materials through this nondestructive method has an extensive range of applications for a wide variety of fields, including quality assessment, industry, and national security.

INTRODUCTION

Every material can be uniquely characterized by its attenuation profile. Developing a nondestructive method that extracts the attenuation profile of any provided material is a challenging problem. Jimenez et. Al. explored the feasibility of extracting these attenuation profiles through various nondestructive methods [1][2][3]. It was determined that the best attenuation profile approximations were achieved by collecting multichannel radiographs of a particular material of interest, and applying an optimization method to this radiography data to estimate its attenuation profile.

The work presented by Jimenez et. Al. was a simulation study in which noise and other potential complications due to the measurement system were ignored. For this work, spectral data was taken and similar estimation methods were applied to the data in order to approximate the attenuation profiles. This work applies spectral data, taken in a laboratory setting, to the previous optimization methods. Therefore, this work aims to validate the work by Jimenez et. Al., while measuring and studying the effects that noise, and other potential complications, will have on the estimation approach. The ability to identify materials quickly and nondestructively through this method has many applications, including uses in national security, inspection, and medicine.

BACKGROUND

Jimenez et. Al. evaluated the feasibility of extracting an attenuation profile with radiographs, and further work explored the best methods of approximation for these profiles. Throughout this work, noise was ignored, and sources and detectors were treated as ideal components. Furthermore, the work with the best approximations used simulated 2D multichannel images with 2000x2000 pixels with 1keV wide bins [1]. The optimization described by Jimenez et. Al. implemented several constraints on the optimization; these constraints worked well for this particular simulation (Figure 1). The optimization was implemented iteratively over a specified energy interval. All these factors were considered in designing a practical experimental design.

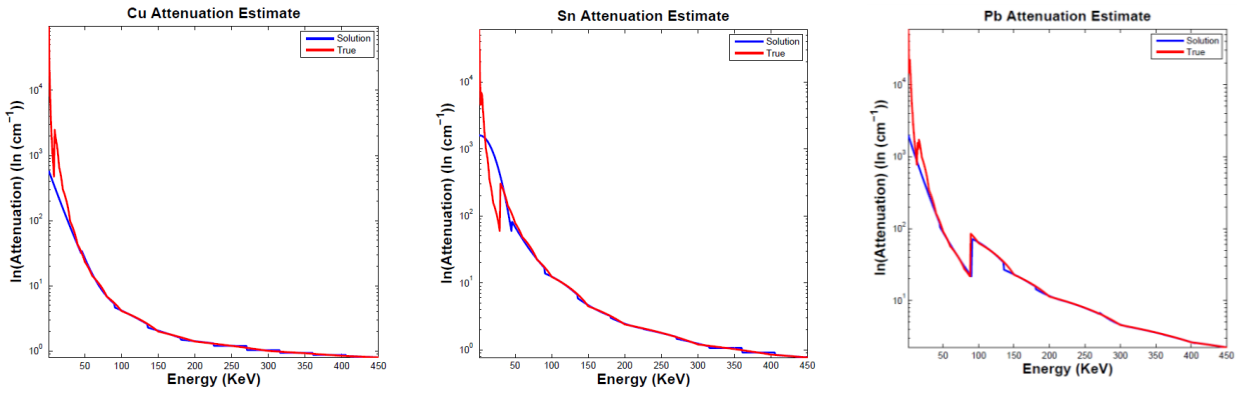

(a) (b) (c)

Figure 1. This shows results from [1]. For the legend on each graph "True" indicates the NIST attenuation profile, and "Solution" indicates the approximation. (a) Copper attenuation estimation compared to NIST profile. (b) Tin attenuation estimation compared to NIST profile. (c) Lead attenuation estimation compared to NIST profile.

APPROACH

The main objective of this work is the ability to classify a material of interest through its radiographic signature. In order to achieve this, the attenuation profile will be estimated, and matched to the corresponding "true" attenuation profile within the National Institute of Standards and Technology database [4]. The first task in achieving this goal is to collect all essential data. First, an "initial spectrum" is obtained. This initial spectrum consists of a Bremsstrahlung x-ray source measurement at the detector location at a given energy (keV) and current (mA) setting. Next, an "attenuated spectrum" is acquired. This measurement consists of the same measurement at the detector and settings, with an additional sheet of material in-between the source and detector.

After collecting these measurements, a direct method as well as an optimization method, similar to that which was done by Jimenez et. Al, is used to extract the attenuation profile of a particular material. The direct method of approximating the attenuation profile uses the initial and attenuated spectrums from a specific material as well as the material's density and thickness, and applies these to Beer's Law (1). Next, the Nelder-Mead optimization method is used to approximate the attenuation profile of a material. This optimization is a simplex optimization [5]. In this study, it searches for the best fitting weighted sum of Legendre polynomial to approximate the attenuation profile. The optimization method uses the same information as the direct method, as well as an initial guess of the attenuation profile. The initial guess is the starting point for the optimization to search from. It continues searching until it minimizes the search function and converges on a solution. In order to evaluate the practicality of this optimization for the chosen experimental design, the optimization will be left unconstrained. This differs from the optimization implemented by Jimenez et. Al [1]. Once this profile is extracted, the results from this work can be compared to the previous simulation work, and the effects of noise can then be evaluated.

IMPLEMENTATION

Equipment

The Amptek XR-100T-CdTe X-Ray and Gamma Ray Detector was used for this work (Figure 2). This detector consists of a single 3 x 3 x 1 mm CdTe pixel. The Amptek detector is an energy discriminating detector. It has energy resolution up to 8192 channels [6]. For the purposes of this work, 1024 channels were used. Additionally, a 3cm thick tungsten collimator with a 500 μm aperture was added to the detector, in order to control the photon flux incident with the detector.

(a) (b)

Figure 2. (a) The Amptek XR-100CdTe X-ray and Gamma Ray Detector with lead bricks (green) used for shielding. (b) Comet 450 keV.

The Amptek detector includes the ADMCA Software, which is the main display and acquisition software for the Amptek detector (Figure 3). All data was collected using the ADMCA software. This software displays the spectrum in real-time during the acquisition, as well as other pertinent metadata such as dead time, total count, input rate, and accumulated time. The ADMCA software also allows users to adjust the gain of the detector. For a given number of channels, the energy width of those channels will depend on the gain specified for the detector. The source used for this work was the Comet 450 keV with a tungsten target. This source is a bremsstrahlung radiation source, with a spot size for the target of 1mm. This source has a voltage range between 20-450 keV, and it supplies a current of from 0.1- 18 mA [7].

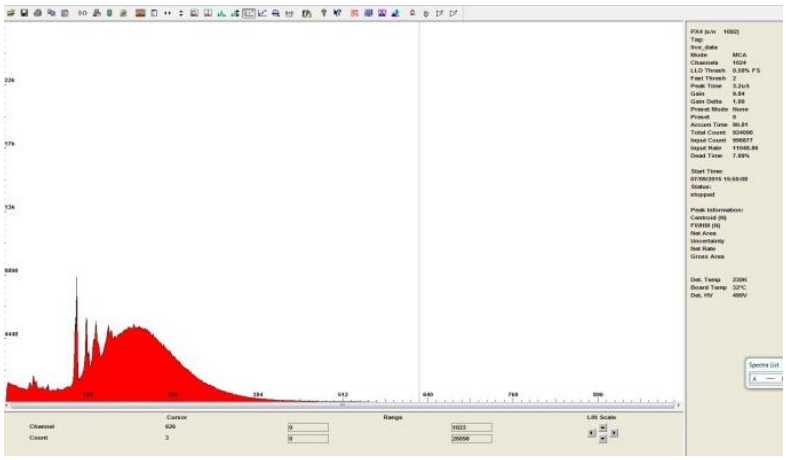

Figure 3. ADMCA display acquisition software

Data Acquisition, Experimental Design and Procedure

The experimental geometry consisted of a source to detector distance of 189cm and a source to object distance of 174cm. The materials used were flat sheets of material, such as lead, tin, copper, titanium, zinc, water, carbon fiber, and polyethylene. In order to align the detector, a laser was first to achieve a rough estimate. Next, the detector was placed on a stage so that it was moved incrementally until the highest input rate on the ADMCA Software was achieved. Once this was accomplished, the detector and source were determined to be aligned. Each initial spectrum and each attenuated spectrum were taken for about 90 seconds. In order to keep the data consistent, the dead time was kept constant at about 10%. To achieve the desired dead time, the current was adjusted accordingly for each acquisition. Additional metadata relevant to the estimation task was also noted in the data file, these include parameters such as source settings (energy and current) as well as material properties (type, thickness, and density). The specific materials emphasized in this work are copper, lead, and tin because these materials were emphasized in the previous work. Consequently, the work from Jimenez et. Al. can be compared to this work and the effects of noise can be evaluated.

Spectrum data was taken up to 450 keV, however, it was determined that the best energy to analyze these spectrums was 100keV. For energies past 100keV the Amptek detector is not adequately efficient [6]. Moreover, at higher energies it is not feasible with our experimental equipment to keep the dead time constant without lowering the current under the desired threshold. When the current is under this threshold, it no longer scales linearly with respect to count rate.

Data Processing

The raw data taken from the Amptek detector had to be normalized in order to be useful (Figure 4). First, the spectrums had to be calibrated in order to assign an energy interval to each channel of the spectrum measurement. Known characteristic tungsten peaks were selected on each spectrum, and an interpolation was done in order to assign an energy interval to each channel on the spectrum. Next, counts outside the energy range the data was taken at were considered to be pulse pileup and deleted. In order to correct for the dead time of the detector, each spectrum was divided by its respective live time. The live time is recorded by the detector with the spectrum measurement. Finally, each spectrum had to be corrected for its current. Each material has a unique density and thickness therefore; different currents were used in order to keep the dead time constant. In order to correct for this, each spectrum was divided by its respective current. Figure 5 shows what the spectrums look like before and after they have been processed.

Figure 4. This flow chart shows the process of normalizing the raw data.

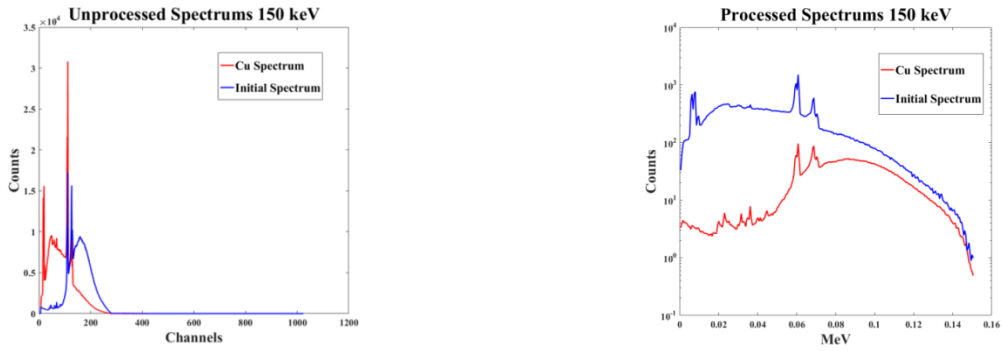

Figure 5. (a) Depicts an initial and the attenuated spectrum for copper, both taken at 150keV, unprocessed. (b) Shows the same spectrums that have been normalized and calibrated.

Direct Method

A direct method was used to approximate the attenuation profile for the materials emphasized in this study. Initial and attenuated spectrums as well as the material density and thicknesses were needed for this calculation. In this method, Beer's Law (1) was applied to the provided information to calculate the attenuation profile. For this calculation, I_{in} is the initial spectrum, I_{out} is the attenuation spectrum, l is the thickness of the material, ρ is the density of the material, and μ is the attenuation profile.

$$\frac{\mu}{\rho} = -\frac{1}{l} \cdot \frac{1}{\rho} \cdot \left(\frac{I_{in}}{I_{out}} \right) \tag{1}$$

Collecting a direct calculation of the attenuation profile is useful because it provides a quick approximation that can be calculated as data is acquired. It can also help determine in the detector is aligned properly. When the detector is not aligned sufficiently, and the direct calculation is applied to the measurements taken, the characteristic peaks (seen in Figure 6 (a) and (c)) are lost. This calculation was done for the materials that are emphasized in this work: tin, copper and lead.

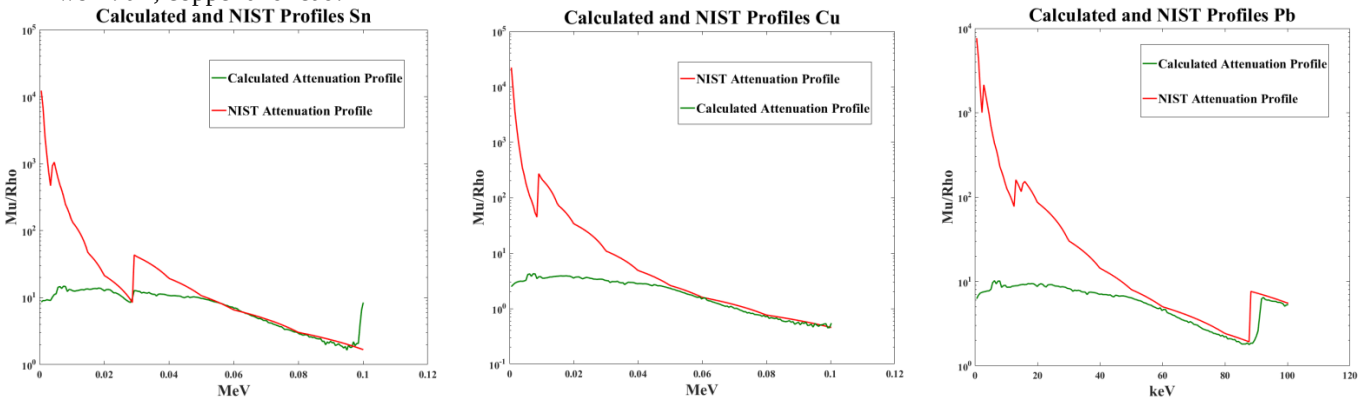

(a) (b) (c)

Figure 6. The direct calculation of the attenuation profile for the materials tested compared to NIST profile. (a) Tin. (b) Copper. (c) Lead.

Optimization

The Nelder-Mead optimization was applied to the experimental data in order to estimate the attenuation profile of each particular material. This optimization inputs the "initial" and "attenuated" spectrums, the material thickness and density, the experimental geometry, and outputs the attenuation profile estimation. Using the experimental geometry and material information, the experiment is modeled in Matlab. This simulation mimics the photons traveling from the source, through the sheet of material, and to the detector. The optimization is given an initial guess of the attenuation profile of the material modeled. The initial guess is represented by a weighted sum of the first five Legendre Polynomials ($\hat{\mu}$). The initial spectrum is input through the simulation and a "synthetic spectrum" $(S_{out})_{is}$ output (2).

$$S_{out} = I_{in} \cdot e^{\hat{\mu} \cdot l} \tag{2}$$

The distance between the synthetic spectrum and the attenuated spectrum is calculated, and the optimization chooses a new attenuation profile estimate, represented by the weighted sum of the Legendre Polynomials, in order to minimize this distance. This process is repeated until the optimization converges and outputs a final attenuation profile estimate. This occurs when the distance between the synthetic spectrum and attenuated spectrum fall below a specified threshold.

The optimization is iterative, and it can be executed over different energy intervals. Figure 7 shows the optimization attenuation estimates for lead performed over differing energy intervals. A single interval was chosen to be the most qualitatively accurate estimate of the attenuation profile. Therefore, Figure 8 shows the single interval optimization estimates for lead, tin and copper. Additionally, the direct calculation estimate is super imposed on these graphs to aid visual comparison.

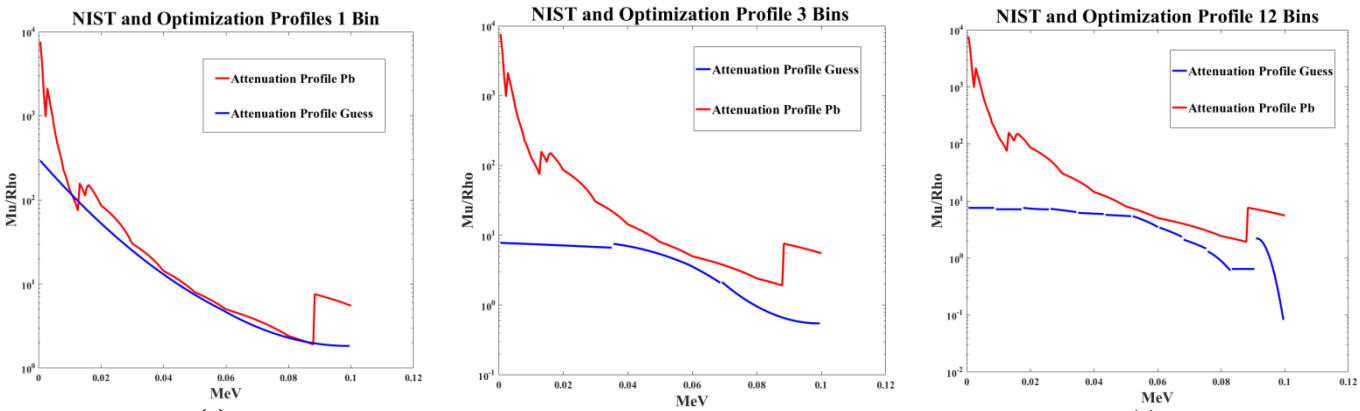

(a) (b) (c)

Figure 7. Optimization attenuation estimates for lead performed over differing energy intervals. (a) A single interval. (b) Three intervals. (c) Twelve intervals

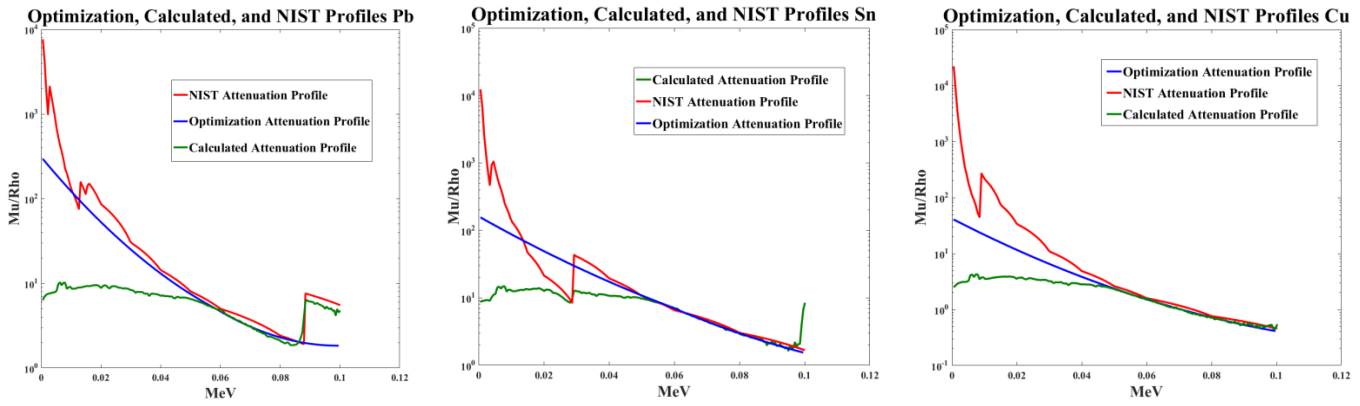

(a) (b) (c)

Figure 8. These graphs show the single interval optimization, direct calculation, and NIST attenuation profiles. (a) Lead. (b) Tin. (c) Copper.

RESULTS

The direct calculation attenuation profile results from Figure 6, indicate that at the lower energy portion of the spectrum, the direct calculation poorly estimates the NIST profile. In the later portion of the spectrum, the direct calculation accurately matches the NIST profile. Finally, the K-edge for lead was resolved most similarly compared to the NIST K-edge; there is some resolve of the K-edge for tin, and none for copper.

Evaluating the optimization iterations in Figure 7, the single interval estimation approximates the entire energy spectrum most accurately compared to the three and twelve interval estimations. For each estimate, the K-edge for lead has been lost. In the case for the twelve interval estimation, the jump in the 12^{th} iteration compared to the pervious iteration could be caused by the K-edge for lead.

Finally, in Figure 8, it is clear that lower energy portions of the energy spectrum are more accurately estimated by the optimization method compared to the direct method. However, the optimization method is unable to resolve the K-edge of any of the materials tested.

DISCUSSION

The results from the direct calculation indicate that this method is able to estimate the attenuation profile more accurately at higher energies. Additionally, the higher Z-value materials' K-edges resolved best; lead resolved the most, and tin resolved slightly. The lowest Z-value material tested was copper, and its K-edge did not resolve. The lower energy portion resolved poorly due to the simplicity of this calculation approach. This method did not accurately account for the amount of photon interactions occurring in the lower portion of the energy spectrum.

Nevertheless, this method is useful because of its ease. It is much less computationally expensive than the optimization method, and it can be used to align the detector.

The optimization method most accurately estimated the general shape of the NIST attenuation profile, however it lacked all characteristic peaks. These peaks were lost due to the nature of the Legendre Polynomials. Legendre Polynomials do not resolve these peaks because they are differentiable functions used to represent the attenuation profile, which contains peaks that are not differentiable. Therefore, when this optimization is left unconstrained, as it was in this study, the K-edges and all other characteristic peaks are lost. Future methods can be implemented to create a better optimization for this problem. For example, the direct calculation for a particular material can be taken, and then used as the initial guess in the optimization. Additionally, a different basis can be used for the optimization instead of the Legendre polynomials. There are a variety of choices, and a basis would be chosen that can accurately model the characteristic peaks in the attenuation profile.

Evaluating the effects of noise compared to work by Jimenez et. Al. was a major focal point in this study. Results from the direct calculation (Figure 6) indicate that noise is a major factor in the low energy portion of the energy spectrum. Both the direct calculation and optimization estimations underestimated the NIST attenuation profile in this portion of the energy spectrum. In future work, sophisticated methods will have to be implemented to compensate for this noise.

CONCLUSIONS

To further this work, a new detector, the Multix ME100, has been purchased by Sandia National Laboratories. The Multix ME100 is a spectroscopic linear detector, with 640 pixels. It provides energy resolution for up to 128 channels, and its energy threshold is 300keV. Figure 9 depicts the spectrum of each pixel from a single line of Multix data. When multiple lines of Multix data are taken a multichannel image can be acquired. Using this multichannel array detector instead of Amptek detector, which consists of a single multichannel pixel, has multiple advantages. It models more accurately the detector simulated by Jimenez et. Al. Additionally, it can efficiently detect higher photon energies (300 keV), also seen in Jimenez et. Al. The completed work described in this paper, as well as future work with the Multix ME 100 detector, provide promise of being able to develop a nondestructive method for comprehensive materials characterization.

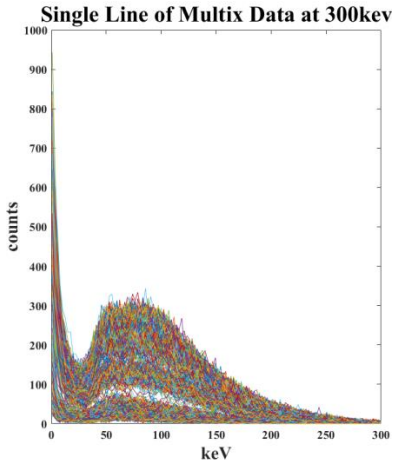

Figure 9. This figure depicts a single line of Multix Data. Each line on the graph represents a pixel on the detector.

ACKNOWLEDGEMENTS

Sandia National Laboratories is a multi-program laboratory managed and operated by Sandia Corporation, a wholly owned subsidiary of Lockheed Martin Corporation, for the U.S. Department of Energy's National Nuclear Security Administration under contract DEAC04-94AL85000.

REFERENCES

[1] E. S. Jimenez, K.R. Thompson, and L.J. Orr, "Object Composition Identification via Mediated-Reality Supplemented Radiographs," in *Nuclear Science Symposium and Medical Imaging Conference*, Oct. 2014.

[2] E. S. Jimenez, K. R. Thompson, and L. J. Orr, "Utilization of virtualized environments for efficient x-ray attenuation approximation," in *ASNT Research Symposium*, Mar. 2014

[3] M. L. M. Edward S. Jimenez, Laurel J. Orr and K. R. Thompson,"Exploring mediated reality to approximate x-ray attenuation coefficients from radiographs," *in Penetrating Radiation Systems and Applications XIV at SPIE Optics+Photonics 2014*, Aug. 2014.

[4] J. Hubbel and S. Seltzer. (2013, Jun.) Tables of x-ray mass attenuation coefficients and mass energy-absorption coefficients from 1 kev to 20 mev for elements z = 1 to 92 and 48additional substances of dosimetric interest. [Online]. Available: http://www.nist.gov/pml/data/xraycoef/

[5] J. A. Nelder and R. Mead, "A simplex method for function minimization," *Computer journal*, vol. 7, no. 4, pp. 308–313, 1965.

[6] X-R-100T-CdTe X-Ray & Gamma Ray Detector. [Online]. Avaliable: http://amptek.com/products/xr-100t-cdte-x-ray-and-gamma-ray-detector/#6

[7] XRS-450. [Online]. http://www.comet-xray.com/Resources/Broschuren/Datenblatt/XRS-450.pdf